Conditions for the Long-Term Preservation of a Deep Brine Reservoir in Ceres

Julie C. Castillo-Rogez[1], M. A. Hesse[2], M. Formisano[3], H. Sizemore[4], M. Bland[5], A. I. Ermakov[1], R. R. Fu[6]

J. C. Castillo-Rogez, Jet Propulsion Laboratory, 4800 Oak Grove Drive, Pasadena, CA 91109, USA (Julie.C.Castillo@jpl.nasa.gov.)

[1]Jet Propulsion Laboratory, California Institute of Technology, Pasadena, CA, United States

[2]The University of Texas at Austin, Department of Geological Sciences, Austin, TX, United States

[3]INAF-IAPS, Istituto di Astrofisica e Planetologia Spaziali di Roma, Italy

[4]Planetary Science Institute, Tucson, AZ, United States

[5]United States Geological Survey, Flagstaff, AZ, United States

[6]Department of Earth and Planetary Sciences, Harvard University, Cambridge, MA, United States

Abstract: We propose a new internal evolution model for the dwarf planet Ceres matching the constraints on Ceres' present internal state from the Dawn mission observations. We assume an interior differentiated into a volatile-dominated crust and rocky mantle, and with remnant brines in the mantle, all consistent with inferences from the Dawn geophysical observations. Simulations indicate Ceres should preserve a warm crust until present if the crust is rich in clathrate hydrates. The temperature computed at the base of the crust exceeds 220 K for a broad range of conditions, allowing for the preservation of a small amount of brines at the base of the crust. However, a temperature $\geq$ 250 K, for which at least 1 wt.% sodium carbonate gets in solution requires a crustal abundance of clathrate hydrates greater than 55 vol.%, a situation possible for a narrow set of evolutionary scenarios.

1. Introduction

Per its combination of chemical, physical, and geological observations on global, regional, and local scales, the Dawn mission has provided the most extensive dataset for an ice-rich body (Russell et al. 2016). Ceres is a 940-km large body with a mean density of 2162 kg/m^3 (Park et al. 2016). This corresponds to an ice to anhydrous rock ratio of 47:53 in volume or 25:75 in mass. Hence its evolution is driven by the interplay of radiogenic heating with the thermodynamic and mechanical properties of water and hydrates. Observational constraints returned by the Dawn mission are summarized in recent studies (e.g., McCord and Castillo-Rogez 2018). The geophysical properties this study aims to match are summarized in Section 2. They include constraints on the properties of the upper 100 km, in particular composition and viscosity profile. An important feature derived from Dawn's observations is a rapid decrease in viscosity within the uppermost 40 km and persistent low viscosities at about 10^{21} Pa s below and at least down to 100 km depth. This has been interpreted by the presence of a few vol.% pore fluid (Fu et al. 2017). Our objective is to determine what set of starting conditions and assumptions on the properties of the crust and potassium distribution enable the preservation of fluids at about 40 km depth until present. Methods are presented in Section 3 and results in Section 4. These results provide thermal context for various processes whose occurrence has been suggested for Ceres, in particular the prospect for cryovolcanism and the development of cryomagma reservoirs upon impact heating in the crust (Hesse and Castillo-Rogez, in revisions) (Section 5). In turn, this study brings new insights into the

internal evolution of a body, which, from a geophysical standpoint, is relevant to other dwarf planets and midsized icy moons.

2. Constraints on Ceres' Interior from Dawn

In the course of two years of orbital mapping, the Dawn mission returned images, near-infrared spectra, and gravity measurements of Ceres on a global scale and for a wide range of illuminations. Gravity data yielded a normalized mean moment of inertia of about 0.37 pointing to partial differentiation (Park et al. 2016). Admittance analysis provided additional constraints on crustal properties, which is 40 km thick on average with a density of 1200 to 1400 kg/m^3 (assuming a two layer model, Ermakov et al. 2017). The crust overlays a mantle with a density of $\sim$2400 kg/m^3 and a viscosity lower than 10^{21} Pa s, which Fu et al. (2017) interpreted as evidence for a small amount of pore fluid. The nature of the fluid is not constrained but it could realistically be sodium and potassium chloride brines as suggested by geochemical modeling (Neveu and Desch 2015; Castillo-Rogez et al. 2018). The brines likely correspond to residual liquid from the freezing of a global ocean suggested in Ceres early on (Castillo-Rogez and McCord 2010; Ammannito et al. 2016). The eutectic temperature of that brine could be as low as about 220 K (Castillo-Rogez et al. 2018). Ammonia could also be present and decrease the eutectic further. However, the widespread occurrence of ammonium both in the form of clays and salts on Ceres' surface indicates these formed in an environment where ammonia was a minor component. Following Le Chatelier's Principle, most of the ammonia should be turned into ammonium since the latter was removed from the medium, either by exchange with cations in clays or by salt precipitation.

Extensive evidence for the occurrence of salt compounds in Ceres' crust is expressed in the form of many sites enriched in carbonates and ammonium chlorides (De Sanctis et al. 2016, 2018). These species are likely associated with other chlorides, like hydrohalite (Castillo-Rogez et al. 2018) that cannot be detected by Dawn's instruments. Brines are believed to play a role in the emplacement of two outstanding geological landmarks: Ahuna Mons (Ruesch et al. 2016) and the bright material (faculae) in Occator crater (De Sanctis et al. 2016; Quick et al. 2019). Both constructs display sodium carbonate (De Sanctis et al. 2016 for the Occator faculae and Zambon et al. 2017 for Ahuna Mons). The deep brine layer identified by Fu et al. (2017) has been suggested as a reservoir for the Occator faculae (Quick et al. 2019).

Additional constraints on Ceres' crustal composition come from its mechanical strength, which Bland et al. (2016) found to be at least three orders of magnitude greater than ice for Ceres' temperatures. It suggests no more than 40 vol.% of a weak phase, which Bland et al. (2016) interpreted as an upper bound on the water ice fraction. That fraction could be less if the crust also contains porosity. The extent of porosity is not constrained though and might show lateral variations, as indicated by the distribution of surface fractures (Scully et al. 2017).

Strong phases are required to reproduce the strength of the crust, which Fu et al. (2017) inferred to be a mixture of phyllosilicates, salt hydrates and gas hydrates (i.e., clathrate hydrates). The latter are likely to be mixed methane and carbon dioxide hydrates (Castillo-Rogez et al. 2018) with a density of about 1000 kg/m^3 (e.g., Waite et al. 2007). Geochemical modeling suggests there should be no more than 20 vol.% salts in

the crust and the averaged density of these salts, composed of carbonates and chlorides is about 2200 kg/m^3 (Castillo-Rogez et al. 2018). In this framework, phyllosilicates are a mixture of magnesium serpentine and clays, in particular saponite, consistent with surface composition (De Sanctis et al. 2015). A mixture of 10 vol.% silicates, 20 vol.% hydrated salts, and 30 vol.% ice and 40 vol.% clathrates matches the average crustal density derived by Ermakov et al. (2017) and is consistent with the strength estimates from Bland et al. (2016) and Fu et al. (2017).

Ceres' crust relaxes on scales greater than ∼250 km, which Fu et al. (2017) interpreted with a crustal viscosity profile decreasing by one order of magnitude every 10 km. Formisano et al. (2018) used a 2-D finite element numerical code to solve the thermal convection equations in the Boussinesq approximation and explore the onset of subsolidus thermal convection in the crust (40 km thick shell) of Ceres. They found that no thermal convection is possible, assuming less than 40vol.% of weak material (Bland et al. 2016). Convection may be possible if the ice content is slightly greater than 40% and the temperature at the base of the crust ranges from 250 to 300 K. Strong thermal convection is possible if 50vol.% of ice is assumed, leading to a Rayleigh number greater than 10^8. However, as shown below, the modeled temperatures at the base of the crust are expected to be colder than required for convection to be initiated throughout Ceres' history.

3. Modeling Approach

This paper follows the one-dimensional thermal modeling approach by Castillo-Rogez and Lunine (2010). We account for the redistribution of potassium following leaching from the silicates upon aqueous alteration. This process is promoted in presence of ammonium

whose exchange with potassium and sodium is enhanced at temperature below 50° C (Neveu et al. 2017). In Castillo-Rogez et al. (2018), potassium accumulates with chlorine and sodium in the residual liquid layer at the base of the crust. The distribution of this brine may encompass a few tens of kilometers in the upper part of the mantle or a larger area depending on porosity. We vary the fraction of potassium leached from the rock from 10 to 90% and redistributed it in the brine layer in the upper part of the mantle, down to the 100 km depth (i.e., the upper 60 km of the mantle) that could be probed by the Fu et al. (2017) modeling.

Ceres is assumed to form about 3.5 Ma after the condensation of calcium and aluminum rich inclusions (CAI) , which define the starting concentrations of ^{26}Al in Ceres. The exact time of formation is not important for this study as long as there is enough ^{26}Al to drive global melting and differentiation following formation. For times of formation later than 5 Ma after CAIs, Castillo-Rogez and McCord (2010) found that Ceres could preserve a thick (>150 km) crust of its original composition, presumably of dry rock. This situation is not consistent with the Dawn observations, both in terms of surface composition, crustal density, and moment of inertia and we do not cover it in the present study.

Freezing occurs top down and results in the development of a crust that is ice rich. Modeling of the freezing of the ocean with FREZCHEM yields salts and clathrates (Castillo-Rogez et al. 2018). Clathrates may represent the dominant form of water at pressures of a few MPa. Hence the crustal composition may range from the minimal 30 vol.% clathrates required by the observations (on top of silicates and hydrated salts) up to 70 vol.%. The thermal conductivity of the mixture, K_{crst}, is the sum of the component conductivities

weighted by their volume fractions. It ranges from about 0.6 W/m/K for 0 vol.% ice (i.e., 70 vol.% clathrates) to 2.0 W/m/K for 55 vol.% ice. Silicates are a minor component of the mixture, and thus their impact on the thermal conductivity is small. This modeling does not account for organics, which might be abundant in the crust (Marchi et al. in press). Organics are diverse and their densities cover a broad range, but their abundance in Ceres' crust is not constrained.

Settling of phyllosilicates upon melting of the ice is assumed to proceed to near completion. That is, we do not model a mudball interior, in which silicate grains remain in suspension with a fluid phase throughout much of the early mantle. The crustal density predicted by Travis et al. (2018) for a mudball interior is broadly consistent with the density inferred from a two-layer gravity model (1450 vs 1290 kg/m^3; Ermakov et al. 2017). The difference might be due to different assumptions on the fraction of rocky particles that can remain in suspension in the ocean. For example ionic charging, a common phenomenon observed in marine clays (e.g., Sutherland et al. 2015) could play a major role in driving particle settling, or flocculation, as the ocean freezes and thus salinity increases. Furthermore, muddy sediment is difficult to erode and resuspend (Hjulstroem 1935). The mudball model predicts the long-term preservation of hundreds of kilometers of liquid inside Ceres at present and, presumably, could match the mechanical constraints derived by Fu et al. (2017). Our admittedly simpler model yields higher heat flow and thus provides a bound on the maximum temperatures that can be reached in Ceres at present. So, the two approaches may be viewed as two endmember evolutionary pathways for Ceres. Lastly, the concentration of metal-rich, i.e., dense, particles toward the center cannot be

ruled out (King et al. 2018). However, the extent of that process is unconstrained, so this study assumes a simple three-layer structure (mantle, briny mud, crust) for Ceres' interior.

Material properties are gathered in the Supplement. For the initial concentration in long-lived radioisotopes, we chose a mean carbonaceous chondrite composition characterized by an average potassium content of $\sim$ 500-550 μg g^{-1} (Lodders 2003). Oceanic muds have a thermal conductivity from 0.5 to $\sim$1.5 W/m/K depending on the relative fractions of particles, brine, gas, and gas hydrates (e.g., Camerlenghi et al. 1995; Muraoka et al. 2014). Serpentine has a thermal conductivity of about 2.5 W/m/K while anhydrous silicates (olivine and pyroxene) have thermal conductivities up to 5 W/m/K (see Opeil et al. 2010 for a review). The latter could be present if aqueous alteration was partial. Also, the presence of iron-rich compounds in the rock (like iron sulfide and oxides) could increase the thermal conductivity further. In this study, we cover a range of thermal conductivities for the mantle from 0.5 to 2.5 W/m/K under the assumption that aqueous alteration was advanced, as suggested by the Dawn observations (e.g., De Sanctis et al. 2018).

4. Representative Interior Evolution Models Consistent with Dawn's Observations

The model presented in Figure 1a is characterized by a mantle thermal conductivity of 1.5 W/m/K, a crust thermal conductivity of 1.1 W/m/K, and assumes 50% of the potassium has been leached from the silicates and is stored in remaining liquid at the top (60 km) of the mantle. In these conditions, the mantle remains cold and never reaches the

dehydration temperature of serpentine and clays, around 800 K. This is consistent with the gravity constraints from Ermakov et al. (2017).

Figure 1b shows the heat flow history for that model. Due to the low conductivity of the core and the insulating effect of the crust, heat leaks out slowly. It slowly decreases over time, from $\sim$ 3 mW/m^2 1 Ga after formation to $\sim$ 2.1 mW/m^2 for present time.

Trends in parametric dependence (Figure 2) show that the key parameter determining the temperature at the base of the crust is, as expected, the crustal thermal conductivity. The mantle thermal conductivity, which determines the heat flowing from the mantle to the crust, further contributes to warming the base, although its impact is at most 12 degrees over a factor five increase. Hence, efficient heat transfer from the mantle combined with an insulating effect of the crust results in trapping heat at the base of the crust and yields temperatures above 220 K (i.e., the eutectic of the chloride brine mixture) for a large space of conditions, specifically if $K_{crst} \leq\sim$ 1.4 W/m/K. The crust-mantle interface temperature reaches the water eutectic for $K_{crst} \leq$ 0.8 W/m/K, whereas an ice-dominated crust with a thermal conductivity $\geq$1.6 W/m/K would not allow temperatures warm enough for brines to persist until present.

The contribution of the displacement of ^{40}K from the rock to a brine layer at the top of the mantle results in increasing the temperature at the interface with the crust by only a few degrees.

A low value of K_{crst} can be explained if the crust is enriched in hydrates, such as clathrate hydrates. A conductivity of 1.4 W/m/K corresponds to about 40 vol.%, which, combined with 20 vol.% salts and 10 vol.% silicates (to meet the observed crustal density),

is consistent with the crustal strength derived by Bland et al. (2016). A value of 0.8 W/m/K, requires $\sim$ 65 vol.% clathrate hydrates, which is theoretically possible but implies that clathrate hydrates formed during the freezing of the ocean avoided destabilization from impacts until. This scenario is hard to reconcile with Ceres' impacting history and with regional evidence for increased ice content in the crust (Sizemore et al., in press.) On the other hand, $K_{crst} \geq 1.6$ W/m/K, the condition for Ceres to be entirely frozen at present, implies an abundance of clathrates $\leq$30%, which is also a plausible scenario. Increased abundance of silicates with respect to hydrated salts, two high strength materials of similar densities but contrasting thermal conductivities, can further act in increasing thermal conductivity.

Temperatures in the modeled mantle exceed the dehydration temperature of hydrated silicates when the average $K_{mtl} \leq 1.2$ W/m/K. The mantle density inferred by Ermakov et al. (2017) indicates little or not hydration of the silicates. It is possible an enrichment in metal-rich particles with depth increases the thermal conductivity of the mantle. An alternative explanation is that hydrothermal circulation could still be ongoing in fractures, enhancing heat transfer and thus the effective thermal conductivity of the medium (Neveu et al. 2015).

The amount of remaining liquid vs. temperature for the mix of salts predicted by Castillo-Rogez et al. (2018) is presented in Figure 3a. The remaining liquid fraction represents $\leq$ 2% of the original ocean for temperatures below $\sim$248 K and $\leq$ 1% below $\sim$244 K. At 220 K, only 0.4% of the original ocean remains. Assuming that all of Ceres' volatile content melted as a consequence of short-lived radioisotope decay (Castillo-Rogez

and McCord, 2010), these fractions correspond to a global layer between 200 m and 1000 m thick. However, below the crust, this liquid is likely distributed in a matrix of silicates and other solid materials in the form of pore (interstitial) fluid down to at least 100 km depth. Further modeling is required to determine the distribution of the liquid based on the expected matrix properties (e.g., porosity and permeability).

5. Implications and Discussion

Our modeling shows that it is realistic from a thermal standpoint to expect at least a few percent of brines (in volume) to be preserved in Ceres' mantle until present, provided that the crust is enriched in insulating material such as clathrates. Clathrates have also been suggested as responsible for the inferred low density and high mechanical strength of the crust (Bland et al. 2016; Fu et al. 2017) and are predicted to be a dominant species from geochemical modeling (Castillo-Rogez et al. 2018). In these conditions, heat flowing from Ceres' crust can be slightly lower than incoming heat from the rocky mantle, which contributes to the long term preservation of liquid. However, unless the crust is dominated by clathrates, Ceres is on the edge of being completely frozen, which is also consistent with Neveu and Desch (2015). On the other hand, as noted above, our modeling approach potentially yields an conservative case where modeling Ceres as a mudball (Travis et al. 2018) could be more appropriate. The bottom line is that the preservation of liquid inside Ceres until present is expected for a wide range of thermal evolution scenarios.

Lateral Variations in Crustal Properties: Sizemore et al. (2018) inferred from Ceres' geology lateral variations in ice content across Ceres. In particular, the Hanami Planum region displays Ceres' most ancient terrains and mildly relaxed geological features in com-

parison to the surrounding planitiae. Most of the craters with central pits are concentrated in this region. Hanami Planum is also characterized by a thicker crust than average ($\sim$ 50 km, Ermakov et al. 2017). A possible interpretation is that this old region has preserved a substantial fraction of clathrates with respect to the planitiae that might represent basins created by large impacts (Marchi et al. 2016). Combining a thicker crust with a low thermal conductivity could then lead to locally warmer temperatures and thus increased abundance in liquid at the base of the crust. Preliminary estimates from this modeling suggest the base of Hanami Planum could be $\sim$5-10 K warmer than the average basal temperature. However, more advanced two- or three- dimensional thermal modeling is required for a more accurate estimate.

The topography relaxation study by Fu et al. (2017) cannot resolve regional variations in viscosity contrast between the crust and mantle. Impact-induced variations in clathrate abundance in the crust could locally shift the crustal thermal conductivity from $\sim$1 W/m/K to up to 2.4 W/m/K, with potential signatures in the geology that remain to be explored.

Prospect for Cryovolcanism: The occurrence of sodium carbonate at both the Occator faculae and Ahuna Mons requires the sources of the constructs to be warm enough for that compound to be in solution. The fluid does not require a large concentration of sodium carbonate though, since the bulk of the Occator dome and of Ahuna Mons could be built from a different material, for example ice shielded from sublimation by a thin crust of carbonate and chlorides.

For our average model, the fraction of $NaHCO_3$ in solution is only 0.1 wt.% at 245 K (Figure 5b). Temperatures in excess of 250 K are required for several percent of that compound to be in solution. Such warm temperatures could be met below Hanami Planum, as noted in the previous subsection. Sodium carbonate is a minor component of the salt inventory modeled for Ceres (e.g., in comparison to the chlorides) and is predicted to be among the first salts incorporated in the crust (Castillo-Rogez et al. 2018). Thus, the extent to which the deep brine layer could represent a major reservoir of sodium carbonate for the Occator faculae is uncertain. An alternative, and potentially complementary scenario is that geological activity associated with Occator and other large craters (in the past) was in part driven by the heat produced upon impacting, as an additional way to inject heat into the crust and put in solution sodium carbonates already present in the crust (Castillo-Rogez et al. 2018) A hybrid model combining both impact-generated melt and a deeper source is another possibility (see next subsection).

Ahuna Mons, a ∼4-km high by 17-km wide construct, sits on a ∼40 km thick crust, similar to our modeling assumption, i.e., temperatures colder than 245 K are expected at the base of the crust.Even in the most optimistic case, the bottom heat flow is lower than 3 mW/m^2, insufficient to drive convective upwelling (Formisano et al., 2018). The lack of flexural deformation associated with the mons further indicates a low heat flow. Instead, Neveu and Desch (2015) suggested that expressions of volcanism on Ceres' surface, such as Ahuna Mons, could be the result of passive upwelling of mantle material due to volume changes in a freezing interior. However, a model that reconciles both mineralogy and geophysics remains to be pursued.

Thermal Context for Impact Melt Production: In the case of the Occator faculae, a cryomagma reservoir produced by impact heat (Bowling et al. 2019; Hesse and Castillo-Rogez, in revisions) can reach the required temperature for a significant fraction of crustal sodium carbonate to get in solution and contribute to the bulk of the facula carbonates as the solution is brought to the surface from freezing stresses (following a similar process as described in Quick et al. 2019). The thermal gradient inferred from our modeling (which favors a certain temperature at the base of the crust), is at least 4 times steeper than the thermal gradient assumed by Bowling et al. (2019) in their modeling of the evolution of the melt reservoir created by the impact that created Occator crater. A different thermal background can have a significant effect over the lifetime of that melt, as pointed out by these authors and demonstrated by Hesse and Castillo-Rogez (in revisions). The latter authors show that the impact-produced melt reservoir could survive up beyond 10 Ma and potentially still be a source for the recent exposure of brines, depending on the size of the impact melt chamber. Our modeling can also be used to compute the amount and depth of melt produced by impacts throughout Ceres' history.

6. Summary

The preservation of a relict ocean in Ceres until present is possible provided that the thermal conductivity of the crust is less than 1.4 W/m/K. This value is consistent with that expected for the mixture of ice and hydrated materials (especially salts and clathrate hydrates) inferred from geophysical observations (Bland et al. 2016; Fu et al. 2017). A moderate rocky mantle thermal conductivity ($\sim 1-2$ W/m/K) further contributes to the preservation of a warm brine layer at the base of the crust. On the other hand,

the displacement of ^{40}K from the rock to the salts has a relatively minor impact on Ceres' crustal temperature. The water ice eutectic is reached if the crust is dominated by clathrate hydrates in excess of 65 vol.%. On the other hand, the prospect of liquid at shallow depth, as depicted in Nathues et al. (2017) and Stein et al. (2017), is unlikely based on our geophysical modeling. This implies that the exposure of salts from a brine reservoir is a phenomenon that might be limited to impacts large enough to connect with the deep brine layer (e.g., via the introduction of fractures) and/or to create a local melt reservoir (Bowling et al. 2019; Hesse and Castillo-Rogez, in revisions). Conversely, the warm thermal background created by a large abundance of hydrates in the crust implies that brine-driven activity following large impacts must have been common in Ceres' history, as illustrated by the many occurrences of salt deposits associated with fracture networks in large craters (Buczkowski et al. 2018; Azacca Crater, Dantu Crater). Clathrates may further contribute to that process by supplying gas when destabilized and increasing melt buoyancy (e.g., Quick et al. 2019).

One cannot exclude that warmer basal temperatures could be reached locally, for example below Hanami Planum's thick crust. Conversely, local conversion of clathrates into ice by large impacts could increase the average crust thermal conductivity, with possible expressions in the surface morphology. Two- or three-dimensional thermal modeling is required to explore the evolution of Ceres' complex crust for comparison against surface features.

Acknowledgments. Part of this work has been conducted at the Jet Propulsion Laboratory, California Institute of Technology, under a contract with NASA. All rights reserved. Government sponsorship acknowledged.

References

Ammannito, E., De Sanctis, M. C., Ciarniello, M., Frigeri, A., Carrozzo, F. G., Combe, J.-Ph., Ehlmann, B. E., et al. (2016) Distribution of ammoniated magnesium phyllosilicates on Ceres, Science 353, aaf4279.

Bland, M. T., Raymond, C. A., Fu, R. R., Schenk, P., Kneissl, T., Pasckert, J.H., Hiesinger, H., Preusker, F., Park, R., Marchi, S., King, S., Castillo-Rogez, J. C., Russell, C.T. (2016), Composition and structure of the shallow subsurface of Ceres revealed by crater morphology, Nature Geoscience 9, 538-542.

Bland, M. T., Sizemore, H. G., Buczkowski, D. L., Sori, M. M., Raymond, C. A., King, S. D., Russell, C. T. (2018a) Why is Ceres Lumpy? Surface Deformation Induced by Solid-State Subsurface Flow, 49th Lunar and Planetary Science Conference 19-23 March, 2018, held at The Woodlands, Texas LPI Contribution No. 2083, id.1627

Bland, M. T., Ermakov, A. I., Raymond, C. A., Williams, D. A., Bowling, T. J., Preusker, F., Park, R. S., Marchi, S., Castillo-Rogez, J. C., Fu, R. R., Russell, C. T. (2018b) Geophys. Res. Lett. 45, 1297-1304.

Bowling, T. J., Ciesla, F. J., Davison, T. M., Scully, J. E. C., Castillo-Rogez, J. C., Marchi, S., Post-Impact Thermal Structure and Cooling Timescales of Occator Crater on Asteroid 1 Ceres, Icarus, https://doi.org/10.1016/j.icarus.2018.08.028.

Buczkowski, D. L., Sizemore, H. G., Bland, M. T., Scully, J. E. C., Quick, L. C., Hughson, K. H. G., Park, R., Preusker, F., Raymond, C. A., Russell, C. T. (2018) Floor?Fractured Craters on Ceres and Implications for Interior Processes, J. Geophys. Res., https://doi.org/10.1029/2018JE005632.

Camerlenghi, A., Cita, M. B., Della Vedova, B., Fusi, N., Mirabile, L., Pellis, G. (1995) Geophysical evidence of mud diapirism on the Mediterranean Ridge accretionary complex, Marine Geophysical Researches 17, 115-141.

Castillo-Rogez, J. C., Lunine, J. I. (2010) Evolution of Titan's rocky core constrained by Cassini observations, Geophysical Research Letters 37, L20205, doi: doi:10.1029/2010GL044398.

Castillo-Rogez, J. C., McCord, T. B. (2010) Ceres' evolution and present state constrained by shape data, Icarus 205, 443-459, doi:10.1016/j.icarus.2009.04.008.

Castillo-Rogez, J. C., Neveu, M., McSween, H. Y., Fu, R. R., Toplis, M., Prettyman, T. H. (2018) Insights into Ceres' evolution from surface composition, Meteoritics and Planetary Science 53, 1820-1843.

Dai, S., Cha, J.-H., Rosenbaum, E. J., Zhang, W., Seol, Y. (2015) Thermal conductivity measurements in unsaturated hydrate-bearing sediments, Geophys. Res. Lett. 42, 6295-6305, doi:10.1002/2015GL064492.

De Sanctis, M. C., Ammanito, E., Raponi, E., Marchi, S., Mcord T. B., et al. (2015) Ammoniated phyllosilicates with a likely outer Solar system origin on (1) Ceres, Nature 528, 241-244.

De Sanctis, M.C., Raponi, A., E. Ammannito, M. Ciarniello, M.J. Toplis, H.Y. McSween, J.C. Castillo-Rogez, B.L. Ehlmann, F.G. Carrozzo, S. Marchi, F. Tosi, F. Zambon, F. Capaccioni, M.T. Capria, S. Fonte1, M. Formisano, A. Frigeri, M. Giardino, A. Longobardo, G. Magni, E. Palomba, L.A. McFadden, C.M. Pieters, R. Jaumann, P. Schenk, R. Mugnuolo, C.A. Raymond, C.T. Russell (2016) Bright carbonate deposits as evidence of aqueous alteration on (1) Ceres, Nature 536, 54-57.12

Engel, S., J. I. Lunine, and D. L. Norton (1994) Silicate interactions with ammonia-water fluids on early Titan, J. Geophys. Res. 99 (E2), 3745-3752.

Ermakov, A. I., Fu, R. R., Castillo-Rogez, J. C., Raymond, C. A., Park, R. S., Preusker, F., Russell, C. T., Smith, D. E., Zuber, M. T., Constraints on Ceres' internal structure and evolution from its shape and gravity measured by the Dawn spacecraft, J. Geophys. Res. 122, 2267-2293.

Formisano, M., Costanzo, F., Magni, G., De Sanctis, M. C. (2018) (1) Ceres: Study of Thermal Convection in the Mantle and its Mechanical Effects, 42nd COSPAR Scientific Assembly. Held 14-22 July 2018, in Pasadena, California, USA, Abstract id. B1.1-20-18.

Fu, R. R., Ermakov, A., Marchi, S., Castillo-Rogez, J. C., and 8 co-authors, Interior structure of the dwarf planet Ceres as revealed by surface topography, EPSL 476, 153-164.

Glein, C. R., Shock, E. L. (2010) Sodium chloride as a geophysical probe of a subsurface ocean on Enceladus, Geophys. Res. Lett. 37, L09204.

Hayne, P. O., Aharonson, O. (2015) Thermal stability of ice on Ceres with rough topography, J. Geophys. Res. 120, 1567-1584.

374 Hesse, M., Castillo-Rogez, J. C., Thermal evolution of the impact-induced cryomagma
375 chamber beneath Occator Crater on Ceres, Geophys. Res. Lett., submitted (provided
376 with submission).

377 Hjulstrom, F. (1935). Studies of the morphological activity of rivers as illustrated by the
378 River Fyris, Bulletin. Geological Institute Upsalsa, 25, 221-527.

379 King S. D., Castillo-Rogez J. C., Toplis M. J., Bland M. T., Raymond C. A., and Russell C.
380 T. 2018. Ceres internal structure from geophysical constraints. Meteoritics & Planetary
381 Science. https://doi.org/10.1111/maps.13063.

382 Kirk, R. L. and D. J. Stevenson (1987) Thermal evolution of a differentiated Ganymede
383 and implications for surface features, Icarus 69, 91-134.

384 Lodders, K. (2003) Solar System Abundances and Condensation Temperatures of the
385 Elements, The Astrophysical Journal 591, 1220, doi:10.1086/375492.

386 Marchi, S., Ermakov, A. I., Raymond, C. A., Fu, R. R., O?Brien, D. P., Bland, M. T.,
387 Ammannito, E., De Sanctis, M. C., Bowling, T., Schenk, P., Scully, J. E. C., Buczkowski,
388 D. L., Williams, D. A., Hiesinger, H., Russell, C. T. (2016) The missing large impact
389 craters on Ceres, Nature Communications 7, Article number: 12257.

390 Marchi, S., Raponi, A., Prettyman, T., De Sanctis, M. C., Castillo-Rogez, J., Raymond,
391 C., Ammannito, E., Bowling, T., Ciarniello, M., Kaplan, H., Palomba, E., Russell,
392 C., Vinogradoff, V., Yamashita, N., An aqueously altered carbon-rich Ceres, Nature
393 Astronomy, in press (embargoed until December 10).

394 McCord T. B. and Castillo-Rogez J. C. (2018). Ceres's internal evolution: The view after
395 Dawn. Meteoritics & Planetary Science. https://doi.org/10.1111/maps.13135.

396 Muraoka, M., Ohtake, M., Susuki, N., Yamamoto, Y., Suzuki, K., Tsuji, T. (2014) Ther-
397 mal properties of methane hydrate?bearing sediments and surrounding mud recovered
398 from Nankai Trough wells, J. Geophys. Res. 119, 8021-8033.

399 Nathues, A., Platz, T., Thangjam, G., Hoffmann, M., Mengel, K., Cloutis, E. A., Le
400 Corre, L., Reddy, V., Kallisch, J., Crown, D. A. (2017) Evolution of Occator Crater on
401 (1) Ceres, Astron. J. 153, 112.

402 Neveu, M. and S. J. Desch (2015) Geochemistry, thermal evolution, and cryovolcanism on
403 Ceres with a muddy mantle, Geophys. Res. Lett. 42, 10,197-10,206.

404 Neveu, M., Desch, S., Castillo-Rogez, J., Aqueous chemistry in icy world interiors: Fate
405 of antifreeze and radionuclides, Geochimica and Cosmochimica Acta 212, 324-371.

406 Opeil, C. P., Consolmagno, C. J., Britt, D. T. (2010) The thermal conductivity of mete-
407 orites: New measurements and analysis, Icarus 208, 449-454.

408 Park, R., Konopliv. A. S., Bills, B. G., Rambaux, N., Castillo-Rogez, J. C., Raymond, C.
409 A., Vaughan, A. T., Ermakov, A. I., Zuber, M. T., Fu, R. R., Toplis, M. J., Russell, C.
410 T., Nathues, A. (2016) Interior structure of dwarf planet Ceres from measured gravity
411 and shape, Nature, accepted.

412 Quick, L., Buzckowski, D. L., Ruesch, O. Scully, J. E. C., Castillo-Rogez, J. C.,
413 Raymond, C. A., Schenk, P. M., Sizemore, H. G., Sykes, M. V., A possible brine
414 reservoir below Occator Crater: Thermal and compositional evolution and forma-
415 tion of the Cerealia Dome and Vinalia Faculae, Occator Special Issue of Icarus,
416 https://doi.org/10.1016/j.icarus.2018.07.016.

417 Ruesch O., Platz, T., Schenk, P., McFadden, L. A., Castillo-Rogez, J. C., et al. (2016)
418 Cryovolcanic activity on Ceres, Science 353, aaf4286.

419 Russell C. T., Raymond C. A., Ammannito E., Buczkowski D. L., De Sanctis M. C.,
420 Hiesinger H., Jaumann R., Konopliv A. S., McSween H. Y., Nathues A., Park R. S.,
421 Pieters C. M., Prettyman T. H., McCord T. B., McFadden L. A., Mottola S., Zuber
422 M. T., Joy S. P., Polanskey C., Rayman M. D., Castillo-Rogez J. C., Chi P. J., Combe
423 J.- P., Ermakov A., Fu R. R., Hoffman M., Jia Y. D., King S. D., Lawrence D. J.,
424 Li J.-Y., Marchi S., Preusker F., Roatsch T., Ruesch O., Schenk P., Villarreal M. N.,
425 Yamashita N. 2016. Dawn arrives at Ceres: Exploration of a small, volatile-rich world.
426 Science 353:1008-1010.

427 Scully, J. E. C., Buczkowski, D. L., Schmedemann, N., Raymond, C. A., Castillo?Rogez,
428 J. C., King, S. D., Bland, M. T., Ermakov, A. I., O'Brien, D. P., Marchi S., Longobardo,
429 A., Russell, C. T., Fu, R. R., Neveu, M. (2017) Evidence for the Interior Evolution of
430 Ceres from Geologic Analysis of Fractures, Geophys. Res. Lett. 44, 9564-9572.

431 Sizemore, H., Schmidt, B., Chilton, H., Hughson, K., Castillo-Rogez, J. C., Sori, M.,
432 Platz, T., Buczkowski, D., Berman, D., Ahrens, C., Scully, J., Crown, D., Schenk,
433 P., Mest, S., Bland, M., Otto, K., Marchi, S., Schorghofer, N., Quick, L., Prettyman,
434 T., De Sanctis, M. C., Nass, A., Thangjam, G., Nathues, A., Raymond, C., Russell,
435 C., A Global Inventory of Ice-Related Morphological Features on Dwarf Planet Ceres,
436 https://doi.org/10.1111/maps.13135.

437 Sori, M. M., Sizemore, H. G., Byrne, S., Bramson, A. M., Bland, M. T., Stein, N. T.,
438 Russell, C. T. (2018) Cryovolcanic rates on Ceres revealed by topography, Nature As-

tronomy, https://doi.org/10.1038/s41550-018-0574-1.

Stein, N. T., Ehlmann, B. L., Palomba, E., De Sanctis, M. C., Nathues, A., Hiesinger, H., Ammannito, E., Raymond, C. A., Jaumann, R., Longobardo, A., Russell, C. T. (2017) The formation and evolution of bright spots on Ceres, Icarus, https://doi.org/10.1016/j.icarus.2017.10.014.

Sutherland, B. R., Barrett, K. J., Gingras, M. K. (2015) Clay settling in fresh and salt water, Environmental Fluid Mechanics 15, 147-160.

Travis B. J., Bland P., Feldman W. C., and Sykes M. (2018) Hydrothermal dynamics in a CM-based model of Ceres. Meteoritics & Planetary Science 53, 2008-2032.

Waite, W. F., Stern, L. A., Kirby, S. H., Winters, W. J., Mason, D. H. (2007) Simultaneous determination of thermal conductivity, thermal diffusivity and specific heat in sI methane hydrate, Geophysical Journal International 169, 767-774, doi:10.1111/j.1365-246X.2007.03382.x.

Zambon, F., Raponi, A., Tosi, F., De Sanctis, M. C., McFadden, L. A., Carrozzo, F. G., Longobardo, A., Ciarniello, M., Krohn, K., Stephan, K., Palomba, E., Pieters, C. M., Ammannito, E., Russell, C. T., Raymond, C. A. (2017) Spectral analysis of Ahuna Mons from Dawn mission's visible?infrared spectrometer, Geophys. Res. Lell. 44, 97-104.

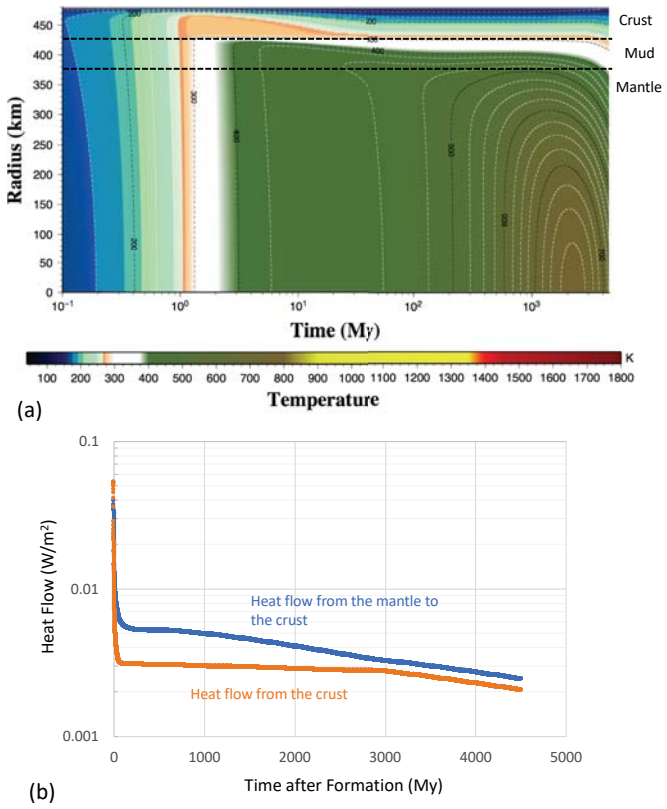

Figure 1. (a) Representative modeling of Ceres' thermal evolution for a time of formation of 3.5 My after the production of Ca-Al inclusions, an averaged crust conductivity of 1.1 W/m/K and mantle thermal conductivity of 1.5 W/m/K. Contour labels are temperatures in Kelvin. The figures display isotherms every 25 K. (b) Corresponding heat flow evolution.

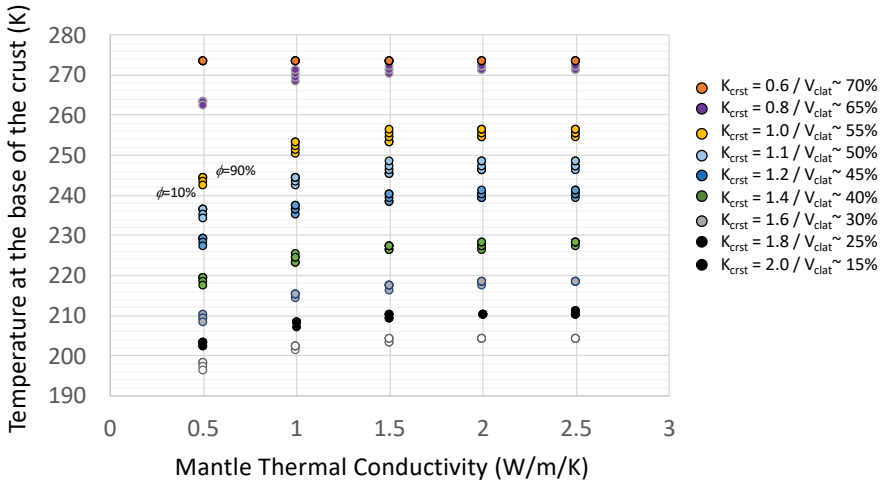

Figure 2. Temperature at the base of the crust as a function of the thermal conductivity in W/m/K of the mantle (assumed constant) and of the crust (temperature dependent, averaged). The corresponding volume fraction of clathrate hydrates in the crust is provided, assuming a mixture of 20 vol.% hydrated salts, 10 vol.%, the rest being ice and clathrates. Point spreads for each model represents the impact of potassium removal from the rock and concentration in a 60 km thick brine layer below the crust, assuming ϕ=0 to 100% transfer of potassium from the rock to the brine.

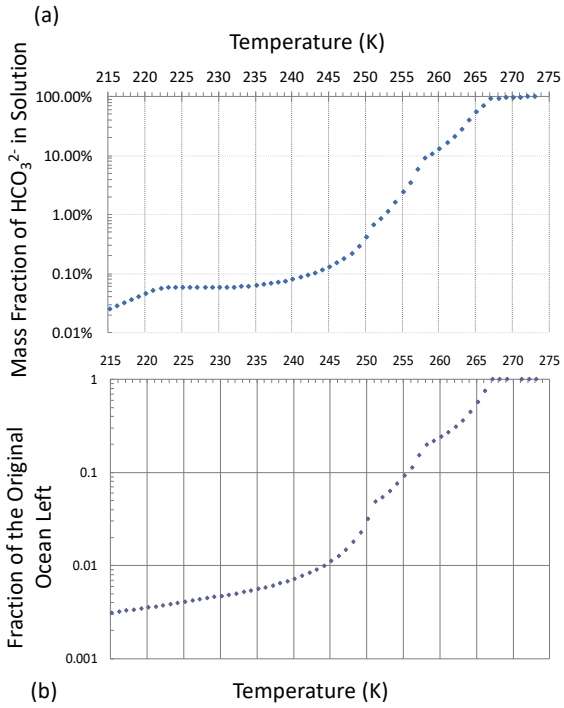

Figure 3. (a) Fraction of liquid left assuming the original ocean was 60 km thick, as a function of the temperature at the base of the crust taking as a reference the ocean composition evolution model from Castillo-Rogez et al. (2018). (b) Fraction of bicarbonate ion in solution as a function of temperature taking as a reference the ocean evolution model from Castillo-Rogez et al. (2018).